

9

Electroweak interactions

One of the most dramatic events in the history of elementary particle physics was the unification of the electromagnetic and the weak interactions into a single, beautiful gauge theory, which was created by Weinberg, Salam and Glashow and which is nowadays referred to as the 'Standard Model' (SM). For a detailed pedagogical account of the need for and development of such a theory, the reader is referred to Leader and Predazzi (1996). We simply recall that this tightly knit theory contains the astounding and incredible prediction of the existence of a set of three vector bosons, W^\pm, Z^0 , with huge masses, $m_W \approx 80 \text{ GeV}/c^2$, $m_Z \approx 90 \text{ GeV}/c^2$, and that these unlikely objects were eventually discovered. (The W was identified at CERN in January 1983 and the Z^0 , also at CERN, a few months later.) A test for the spin of the W is described in subsection 8.2.1(ix).

In the Standard Model the electroweak interactions are mediated by the exchange of photons, Z s and W s, whose coupling to the basic fermions (leptons and quarks) is a mixture of vector and axial-vector. To begin with all particles are massless, and their masses are generated by spontaneous symmetry breaking. The usual mechanism of symmetry breaking requires a neutral scalar particle, the Higgs meson H , whose mass is not determined by the theory. H has not yet been detected experimentally and is the most serious missing link in the theory. But in every other respect the theory has been remarkably successful. All the first-generation experimental tests have been passed with flying colours and a new generation of more refined and demanding tests has been carried out at the two highest energy e^+e^- colliding beam machines, LEP at CERN and SLC at Stanford. It has been realized that some of the cleanest tests involve spin-dependent measurements and SLC has made excellent use of such ideas. Some work on polarized e^\pm beams has been done at LEP, but the push for higher energies and the use of LEP in the construction of the new large hadron

collider (LHC) means that a detailed spin programme was never carried out.

We shall recall the essential elements of the SM and then concentrate on the spin-dependent possibilities.

9.1 Summary of the Standard Model

There are three generations of leptons, (e^-, ν_e) , (μ^-, ν_μ) , and (τ^-, ν_τ) and the neutrinos are treated as massless. The charged lepton fields, which we designate by the symbol for the particle, are split into left- and right-handed parts, see eqns (4.6.53), (4.6.54), and the neutrinos are, by definition, left-handed.

The left-handed parts are grouped into *weak isospin* doublets

$$\begin{pmatrix} \nu_e \\ e \end{pmatrix} \quad \begin{pmatrix} \nu_\mu \\ \mu^- \end{pmatrix} \quad \begin{pmatrix} \nu_\tau \\ \tau^- \end{pmatrix}$$

and the charged bosons W^\pm interact universally with these. Interactions involving W^\pm are called *charged current* interactions and these only involve left-handed leptons. The relevant part of the interaction Lagrangian density has the following form:

$$\mathcal{L}_{W\text{-lept}} = \frac{e}{2\sqrt{2} \sin \theta_W} \left\{ \left[\bar{\nu}_e \gamma^\mu (1 - \gamma_5) e W_\mu + \bar{e} \gamma^\mu (1 - \gamma_5) \nu_e W_\mu^\dagger \right] + \mu^- \text{ terms} + \tau^- \text{ terms} \right\}. \tag{9.1.1}$$

Here e is the magnitude of the electron charge and θ_W , the Weinberg angle, is a crucial parameter in the unifying of the weak and electromagnetic interactions.

The above interaction gives rise to the following Feynman diagram vertices:

$$W^\pm \text{ vertex} = \frac{ie}{2\sqrt{2} \sin \theta_W} \gamma^\mu (1 - \gamma_5) \tag{9.1.2}$$

where the arrow shows the flow of fermion number or, equivalently, lepton number. Identical vertices occur for μ^\pm and τ^\pm .

The form of the W -propagator depends upon the gauge choice. It is simplest in what is called the unitary gauge:

$$\mu \text{ --- } k \text{ --- } \nu = \frac{i \left(-g_{\mu\nu} + k_\mu k_\nu / m_W^2 \right)}{k^2 - m_W^2 + i\epsilon}. \tag{9.1.3}$$

Note, in (9.1.1), that only left-handed leptons are annihilated but also, because $\gamma^\mu(1 - \gamma_5) = (1 + \gamma_5)\gamma^\mu$, that only left-handed leptons are created. This follows since, from (4.6.53),

$$\bar{u}_L = u_L^\dagger \gamma^0 = \left[\frac{1}{2}(1 - \gamma_5)u \right]^\dagger \gamma^0 = \bar{u} \frac{1}{2}(1 + \gamma_5).$$

The Z^0 , which gives rise to *neutral current* weak interactions, interacts with a superposition of left- and right-handed charged leptons. The relevant part of the interaction Lagrangian density is

$$\mathcal{L}_{Z\text{-lept}} = e \{ [\bar{e}\gamma^\mu(v_e - a_e\gamma_5)eZ_\mu + \bar{\nu}_e\gamma^\mu(v_\nu - a_\nu\gamma_5)\nu_eZ_\mu] + \mu^- \text{ terms} + \tau^- \text{ terms} \}. \tag{9.1.4}$$

where, for a fermion f ,

$$v_f = \frac{I_3^f - 2Q_f \sin^2 \theta_W}{2 \sin \theta_W \cos \theta_W}$$

$$a_f = \frac{I_3^f}{2 \sin \theta_W \cos \theta_W}. \tag{9.1.5}$$

Here I_3^f and Q_f are the third component of weak isospin and the charge (in units of e) of the fermion. Thus

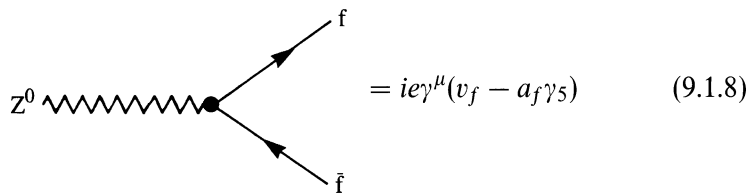
$$v_e = \frac{-1 + 4 \sin^2 \theta_W}{4 \sin \theta_W \cos \theta_W} \quad a_e = \frac{1}{4 \sin \theta_W \cos \theta_W} \tag{9.1.6}$$

and

$$v_{\nu_e} = \frac{1}{4 \sin \theta_W \cos \theta_W} = a_{\nu_e}. \tag{9.1.7}$$

Note that because $\sin^2 \theta_W \approx 0.23$ one finds that $v_e \ll a_e$, so that the coupling to the charged leptons is almost purely axial-vector.

The Feynman diagram vertices are



with identical vertices for the generations e, μ, τ .

A fascinating feature of the theory is the interference between Z^0 and photon exchange, so we recall that the standard QED vertex is

$$= ie\gamma^\mu \tag{9.1.9}$$

with identical vertices for μ^\pm, τ^\pm .

The Z^0 and photon propagators are

$$= \frac{i(-g_{\mu\nu} + k_\mu k_\nu / m_Z^2)}{k^2 - m_Z^2 + i\epsilon} \tag{9.1.10}$$

$$= \frac{-ig_{\mu\nu}}{k^2 + i\epsilon} \tag{9.1.11}$$

For all fermions, the propagators are

$$= \frac{i}{\not{p} - m + i\epsilon} \tag{9.1.12}$$

where \not{p} is the momentum flow in the direction of the fermion number-flow arrow.

Because interference effects between different diagrams are so interesting, care must be taken to allow for possible relative signs between diagrams; these signs arise from the sequential order of the fermionic operators that occur in the products of operators responsible for the diagrams.

Some of the most beautiful effects arise because (9.1.1) and (9.1.4) contain a mixture of vector and axial-vector coupling and thus do not conserve parity.

The parameter θ_W fixes the relative couplings of γ, Z, W to charged leptons, but even to the lowest order in perturbation theory, it plays several other rôles as well (see Chapter 4 of Leader and Predazzi (1996)).

The Higgs mechanism, which gives mass to W^\pm and Z , results in the relation

$$m_W = m_Z \cos \theta_W \tag{9.1.13}$$

and a computation of the muon lifetime in $\mu^- \rightarrow e^- + \bar{\nu}_e + \nu_\mu$ relates θ_W and m_W to the Fermi coupling constant $G \equiv G_F \equiv G_\mu$:

$$m_W = \left(\frac{\pi\alpha}{\sqrt{2}G} \right)^{1/2} \frac{1}{\sin \theta_W} \tag{9.1.14}$$

where α is the fine structure constant.

The coupling of the vector bosons to quarks is analogous to the leptons except that Cabibbo–Kobayashi–Maskawa generation mixing takes place and there is universal coupling to the three left-handed doublets

$$\begin{pmatrix} u_1 \\ d'_1 \end{pmatrix}_L \equiv \begin{pmatrix} u \\ d' \end{pmatrix}_L \quad \begin{pmatrix} u_2 \\ d'_2 \end{pmatrix}_L \equiv \begin{pmatrix} c \\ s' \end{pmatrix}_L \quad \begin{pmatrix} u_3 \\ d'_3 \end{pmatrix}_L \equiv \begin{pmatrix} t \\ b' \end{pmatrix}_L$$

where

$$\begin{pmatrix} d' \\ s' \\ b' \end{pmatrix}_L = V \begin{pmatrix} d \\ s \\ b \end{pmatrix}_L \tag{9.1.15}$$

or

$$d'_i = V_{ij}d_j \tag{9.1.16}$$

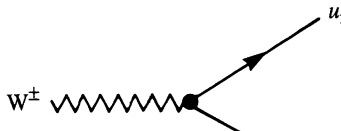
and V is the 3×3 unitary Kobayashi–Maskawa matrix.

Although its existence had more or less been taken for granted, on account of its rôle in calculations that agreed with a host of data, the top quark t was discovered only in 1994, at Fermilab. Its mass has turned out to be somewhat larger than originally expected: $m_t \approx 175 \text{ GeV}/c^2$.

The relevant parts of the Lagrangian density for the charged current interactions are:

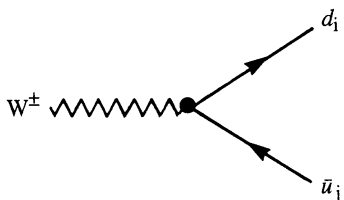
$$\mathcal{L}_{W\text{-quark}} = \frac{e}{2\sqrt{2} \sin \theta_W} \left\{ \left[\bar{u}\gamma^\mu(1 - \gamma_5)d' W_\mu + \bar{d}'\gamma^\mu(1 - \gamma_5)u W_\mu^\dagger \right] + c, s' \text{ term} + t, b' \text{ term} \right\}. \tag{9.1.17}$$

This gives rise to the following Feynman diagram vertices



The diagram shows a wavy line representing a W^\pm boson entering a vertex from the left. From this vertex, two fermion lines emerge: one pointing up and to the right labeled u_i , and one pointing down and to the right labeled d'_j .

$$= \frac{ieV_{ij}}{2\sqrt{2} \sin \theta_W} \gamma^\mu(1 - \gamma_5) \tag{9.1.18}$$



The diagram shows a wavy line representing a W^\pm boson entering a vertex from the left. From this vertex, two fermion lines emerge: one pointing up and to the right labeled d_i , and one pointing down and to the right labeled \bar{u}_j .

$$= \frac{ieV_{ij}^\dagger}{2\sqrt{2} \sin \theta_W} \gamma^\mu(1 - \gamma_5). \tag{9.1.19}$$

For the neutral current interactions there is no generation mixing and the coupling to $q\bar{q}$ has exactly the same structure as for the lepton–antilepton pairs, as given in (9.1.4) and (9.1.5), where now I_3^f and Q_f refer to the quark weak isospin and charge. The vertices are thus shown in (9.1.8).

Of course when dealing with quarks one must remember that all the above applies equally to each quark colour.

In addition to the above there are interaction terms involving the Higgs meson coupling to fermions and to the vector mesons and the self-coupling of the vector mesons. None of these is directly relevant to our study, which will deal mainly with fermionic reactions, but of course they will play a rôle in higher-order perturbative corrections. The detailed Feynman rules can be found in Appendix 2 of Leader and Predazzi (1996).

The Higgs meson does contribute to the reactions we shall consider, but its effect, in lowest order, is negligible because of the weakness of the coupling to fermions:

$$= -i (\sqrt{2}G)^{1/2} m_f I. \quad (9.1.20)$$

This is especially small for reactions at LEP and SLC, where f in the initial state is always an electron. Note, from (9.1.14), that

$$(\sqrt{2}G)^{1/2} m_f = \left[\frac{(\pi\alpha)^{1/2}}{\sin \theta_W} \right] \left(\frac{m_f}{m_W} \right).$$

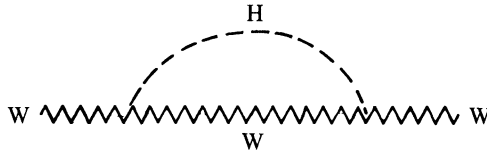
Higgs exchange will be ignored in the following.

9.2 Precision tests of the Standard Model

The properties of many experimental reactions have been calculated in lowest-order perturbation theory (the Born or tree approximation); they are all consistent with the results of the first generation of experiments carried out in the past few years. In particular the parameter θ_W occurs in many different situations and its various determinations are all mutually consistent.

There is now great interest in testing the deeper quantum-field-theoretic aspects of the theory by comparing precision experiments with calculations done to higher order. (Recall the seminal rôle of the Lamb shift and $g - 2$ for QED!) But the procedure is not quite straightforward, given the non-discovery thus far of the Higgs, because while at the Born level we can simply deal with reactions that do not involve it, in higher orders it is unavoidable. For example, although the Higgs couples very weakly to light fermions, its coupling to the vector bosons (which is dimensionless) is effectively large, $2(\sqrt{2}G)^{1/2}m_W^2$, so that its contribution to the W

propagator,



is important.

Thus the detailed higher-order corrections will depend upon the unknown parameter m_H and it becomes very interesting to look for observables that are particularly sensitive to this parameter.

Finally, in going to higher orders, because of infinite renormalization effects one has to decide more carefully what exactly the parameters are that go into the perturbative calculations.

A natural set to use would be α , m_W , m_Z and m_t , m_H , but m_W is less accurately known on account of the neutrino involved in its decay. To obviate this problem one can compute the rate for $\mu^- \rightarrow e^- + \bar{\nu}_e + \nu_\mu$ to order α^2 , in which case (9.1.14) is altered to

$$m_W^2 = \left(\frac{\pi\alpha}{\sqrt{2}G} \right) \left(\frac{1}{\sin^2 \theta_W} \right) \frac{1}{1 - \Delta r} \tag{9.2.1}$$

where Δr is a calculated correction of order α , whose precise value depends upon the renormalization scheme used.

If one chooses a scheme where (9.1.13) holds exactly (the so-called ‘on-shell’ scheme), i.e. θ_W is defined by

$$\cos \theta_W \equiv \frac{m_W}{m_Z}, \tag{9.2.2}$$

then one can use the fact that G is known to great accuracy,

$$G = 1.66389(22) \times 10^{-5} \left(\text{GeV}/c^2 \right)^2, \tag{9.2.3}$$

and take α , G and m_Z as basic parameters. Now m_W and θ_W are calculated from (9.2.1) and (9.2.2), i.e.

$$\cos^2 \theta_W \sin^2 \theta_W = \left(\frac{\pi\alpha}{\sqrt{2}Gm_Z^2} \right) \frac{1}{1 - \Delta r} \tag{9.2.4}$$

and

$$m_W^2 = m_Z^2 \cos^2 \theta_W. \tag{9.2.5}$$

The dominant contribution to Δr is

$$\Delta r \approx \Delta\alpha - \frac{3}{8\sqrt{2}\pi^2} \frac{\cos^2 \theta_W}{\sin^2 \theta_W} Gm_t^2$$

where $\Delta\alpha$ is a QED correction, $\Delta\alpha \simeq 0.064$.

It is estimated that the error in the calculation of Δr arising from imperfectly controlled hadronic physics implies an uncertainty in $\sin^2 \theta_W$ as calculated from (9.2.4) of

$$\delta(\sin^2 \theta_W) = \pm 0.0004. \quad (9.2.6)$$

This then sets a fantastic goal for the accuracy in the new generation of measurements; thus one should look for other reactions in which $\sin^2 \theta_W$ plays such a sensitive rôle that it can be measured to the accuracy (9.2.6).

The most promising approach seems to be via the measurement of the vector part of the Z coupling to fermion–antifermion pairs, i.e. of v_f , defined in (9.1.5). But because v_f is so small it is essential to look for parity-violating effects, where interference between vector and axial-vector couplings will give rise to observables proportional to $v_f a_f$ rather than to $v_f^2 + a_f^2$ as in parity-conserving quantities.

Several reactions seem possible, but by the far the most sensitive to $\sin^2 \theta_W$ are those involving forward–backward asymmetries using longitudinally polarized e^\pm beams, and those involving measurement of the polarization of the final state fermion. In order to optimize the event rate the e^+e^- energy should be close to the Z^0 peak.

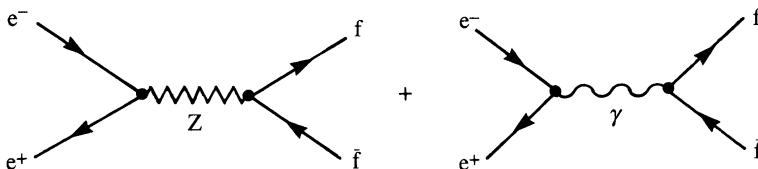
To evaluate the dominant dependence on $\sin^2 \theta_W$ it will be sufficient to discuss the reaction in the Born approximation but, clearly, in the eventual comparison between theory and experiment the theoretical predictions must include higher-order effects. (These are described in detail in Consoli and Hollik (1989).)

9.2.1 The reaction $e^-e^+ \rightarrow \text{fermion–antifermion pair}$

Consider the process

$$e^-e^+ \rightarrow f\bar{f}$$

in the region of the Z peak,¹ so that we can ignore photon exchange, for simplicity, with longitudinally polarized electrons and positrons; here f is any lepton. At the huge energies involved $m/E \ll 1$ for all the fermions involved, so that, as discussed in subsection 4.6.3, helicity and chirality are indistinguishable. The lowest-order diagrams are:



¹ Parameters evaluated at the Z energy are sometimes called the ‘pole parameters’ and are given a superscript 0

Because the energy is close to the Z^0 mass it is not adequate to use the propagator given in (9.1.10) and a more realistic version that takes into account the finite width Γ_Z of the Z must be used:

$$\mu \overset{k}{\text{Z}} \nu = \frac{i(-g_{\mu\nu} + k_\mu k_\nu / m_Z^2)}{k^2 - m_Z^2 + ik^2 \Gamma_Z / m_Z} \quad (k^2 \approx m_Z^2). \quad (9.2.7)$$

The contribution from γ exchange is of order Γ_Z / m_Z compared with Z exchange, which will be neglected in our qualitative discussion. It could be included easily. In fact we will not actually evaluate the Feynman diagrams but derive the results in a fashion that highlights the physical ingredients. Thus we shall view the process as a physical process of resonance formation and decay,

$$e^- e^+ \rightarrow Z \rightarrow f \bar{f}.$$

From subsection 8.2.1, the amplitude is of the form

$$H_{f\bar{f};e\bar{e}}(\theta) = M(f, \bar{f})M(e, \bar{e})d_{\lambda\mu}^1(\theta) \quad (9.2.8)$$

$$\lambda = e - \bar{e} \quad \mu = f - \bar{f},$$

where, because we shall be interested only in ratios of cross-sections at the same energy, we have left out a function of energy related to the behaviour of the Z propagator. The labels in (9.2.8) refer to the helicities of the relevant particles and the M s measure the amplitudes for $e^- e^+ \rightarrow Z$ and $f \bar{f} \rightarrow Z$ respectively.

We know from subsection 4.6.2 that the fermions and antifermions must have opposite helicity, so only two decay amplitudes occur, $M(+, -)$ and $M(-, +)$. Moreover if in (9.1.8) we write

$$v - a\gamma_5 = \frac{1}{2}(v + a)(1 - \gamma_5) + \frac{1}{2}(v - a)(1 + \gamma_5) \quad (9.2.9)$$

we see that apart from irrelevant normalization we can take

$$M(+, -) = v - a \quad M(-, +) = v + a. \quad (9.2.10)$$

The only helicity amplitudes are then

$$\begin{aligned} H_{+-;+-} &= (v_f - a_f)(v_e - a_e)d_{11}^1(\theta) \\ H_{-+;-+} &= (v_f + a_f)(v_e + a_e)d_{-1-1}^1(\theta) \\ H_{+-;-+} &= (v_f - a_f)(v_e + a_e)d_{-11}^1(\theta) \\ H_{-+;+-} &= (v_f + a_f)(v_e - a_e)d_{1-1}^1(\theta) \end{aligned} \quad (9.2.11)$$

where

$$d_{11}^1(\theta) = d_{-1-1}^1(\theta) = \frac{1}{2}(1 + \cos \theta)$$

and

$$d_{1-1}^1(\theta) = d_{-11}^1(\theta) = \frac{1}{2}(1 - \cos \theta).$$

The unpolarized differential cross-section has the simple form, in the CM frame,

$$\frac{d\sigma}{d\Omega} = \frac{3}{16\pi} \sigma \left[1 + \cos^2 \theta + 2\mathcal{A}_f \mathcal{A}_e \cos \theta \right] \tag{9.2.12}$$

where

$$\mathcal{A}_i \equiv \frac{2v_i a_i}{v_i^2 + a_i^2} \tag{9.2.13}$$

is a direct measure of the vector coupling v_i and σ is the total integrated cross-section.

The most general experiment possible in $e^-e^+ \rightarrow f\bar{f}$ is described by eqn (5.6.3). Since we are looking for parity-violating effects we consider longitudinally polarized e^\mp . Let $\mathcal{P}_e, \mathcal{P}_{\bar{e}}$ be the degree of longitudinal polarization of the e^-, e^+ beams respectively in their helicity rest frames, as depicted in Fig. 3.1 for particles A and B , so that, for both e^\mp ,

$$\mathcal{P} = \frac{n_R - n_L}{n_R + n_L}$$

where $n_{R,L}$ are the relative numbers of right- and left-handed particles. Then the initial state density matrix is determined by

$$\mathcal{P}_e = (0, 0, \mathcal{P}_e) \quad \text{and} \quad \mathcal{P}_{\bar{e}} = (0, 0, \mathcal{P}_{\bar{e}}). \tag{9.2.14}$$

Because of the simple structure of the helicity amplitudes (9.2.11), the CM reaction parameters defined in (5.6.4) are easily evaluated. Those that interest us are independent of ϕ , as follows from (5.6.2) and (5.3.3). One has:

- the electron longitudinal analysing power,

$$\begin{aligned} A_Z(\theta) &\equiv A_Z(e^-) = (Z0|00) \\ &= -\frac{\mathcal{A}_e(1 + \cos^2 \theta) + \mathcal{A}_f(2 \cos \theta)}{1 + \cos^2 \theta + \mathcal{A}_e \mathcal{A}_f(2 \cos \theta)} \end{aligned} \tag{9.2.15}$$

$$= -A_Z(e^+); \tag{9.2.16}$$

- the initial state correlation parameter,

$$A_{ZZ} \equiv (ZZ|00) = -1. \tag{9.2.17}$$

Equation (9.2.17) is a direct signature of the fact that only electrons and positrons of opposite helicity can interact with each other.

Using these in (5.6.3) yields

$$\begin{aligned} \frac{d\sigma}{d\Omega}(\mathcal{P}_e, \mathcal{P}_{\bar{e}}) &= \frac{d\sigma}{d\Omega} [(1 - \mathcal{P}_e \mathcal{P}_{\bar{e}}) + (\mathcal{P}_e - \mathcal{P}_{\bar{e}})A_Z(\theta)] \\ &= \frac{3\sigma}{16\pi} \left\{ [1 - \mathcal{P}_e \mathcal{P}_{\bar{e}} + \mathcal{A}_e(\mathcal{P}_e - \mathcal{P}_{\bar{e}})] (1 + \cos^2 \theta) \right. \\ &\quad \left. + \mathcal{A}_f [\mathcal{A}_e(1 - \mathcal{P}_e \mathcal{P}_{\bar{e}}) + \mathcal{P}_{\bar{e}} - \mathcal{P}_e] 2 \cos \theta \right\} \end{aligned} \tag{9.2.18}$$

Thus

$$\frac{d\sigma}{d\Omega}(\mathcal{P}_e, \mathcal{P}_{\bar{e}}) = \frac{3\sigma}{16\pi} \left[(1 + \gamma_1)(1 + \cos^2 \theta) + \mathcal{A}_f(\mathcal{A}_e + \gamma_2)2 \cos \theta \right] \tag{9.2.19}$$

where

$$\gamma_1 \equiv -\mathcal{P}_e \mathcal{P}_{\bar{e}} + \mathcal{A}_e(\mathcal{P}_e - \mathcal{P}_{\bar{e}}) \quad \gamma_2 \equiv \mathcal{P}_{\bar{e}} - \mathcal{P}_e - \mathcal{P}_e \mathcal{P}_{\bar{e}} \mathcal{A}_e. \tag{9.2.20}$$

For the integrated cross-section we have

$$\sigma(\mathcal{P}_e, \mathcal{P}_{\bar{e}}) = \sigma \{1 - \mathcal{P}_e \mathcal{P}_{\bar{e}} + \mathcal{A}_e(\mathcal{P}_{\bar{e}} - \mathcal{P}_e)\}. \tag{9.2.21}$$

(i) *The left-right asymmetry A_{LR}*

Let σ_L and σ_R be the integrated cross-section for the interaction of left and right-handed electrons respectively with unpolarized positrons. Then from (9.2.21) we have

$$A_{LR} \equiv \frac{\sigma_L - \sigma_R}{\sigma_L + \sigma_R} \tag{9.2.22}$$

$$= \mathcal{A}_e \quad \text{in the Born approximation.} \tag{9.2.23}$$

Taking $\sin^2 \theta_W = 0.23$ yields $\mathcal{A}_e = 0.16$.

When higher-order corrections are taken into account the relationship (9.2.23) will change only slightly, because the radiative corrections largely cancel in the asymmetry. The structure of (9.2.21) remains the same but with \mathcal{A}_e replaced by A_{LR} , i.e.

$$\sigma(\mathcal{P}_e, \mathcal{P}_{\bar{e}}) = \sigma [1 - \mathcal{P}_e \mathcal{P}_{\bar{e}} + A_{LR}(\mathcal{P}_{\bar{e}} - \mathcal{P}_e)]. \tag{9.2.24}$$

As discussed in subsection 7.2.1 this could have been used to *measure* $\mathcal{P}_e, \mathcal{P}_{\bar{e}}$ and A_{LR} by running LEP in the four polarization settings:

$$(\mathcal{P}_e, \mathcal{P}_{\bar{e}}) = (0, 0), (\mathcal{P}_e, 0), (0, \mathcal{P}_e), (\mathcal{P}_e, \mathcal{P}_{\bar{e}}).$$

If it were possible to have 50% polarization and 10^6 events the statistical precision on A_{LR} would be $\delta A_{LR} = 0.002$, leading to $\delta(\sin^2 \theta_W) \approx 0.0004$.

Now that m_t is reasonably well determined, a measurement of A_{LR} to the above accuracy will quite strongly constrain the possible values of m_H .

The most advanced studies thus far have been carried out by the SLD collaboration at the SLC at Stanford (see Prepost, 1996). Although using only 93 000 events at the Z^0 mass, the beam polarization \mathcal{P}_e is known with great accuracy to be $(77.23 \pm 0.52)\%$ and A_{LR} is measured with amazing precision:

$$A_{LR} = 0.1543 \pm 0.0039. \tag{9.2.25}$$

Allowing for the higher-order radiative corrections, this result is expressed as a value for $\sin^2 \theta_W^{\text{eff}}$, which differs from $\sin^2 \theta_W$ defined in (9.2.2) by small radiative corrections (see Hollik, 1990). The result is

$$\sin^2 \theta_W^{\text{eff}} = 0.23060 \pm 0.00050, \tag{9.2.26}$$

making it the world's most precise determination of θ_W^{eff} from a single experiment.

(ii) *The forward–backward asymmetry A_{FB}*

It is clear from (9.2.19) that a forward–backward asymmetry exists (i.e. under $\theta \rightarrow \pi - \theta$) because of the term linear in $\cos \theta$ and that this is non-zero because of interference between vector and axial-vector terms. The forward–backward asymmetry A_{FB} is defined as

$$A_{FB} = \frac{n_F - n_B}{n_F + n_B} \tag{9.2.27}$$

where $n_{F,B}$ are the numbers of events in the forward and backward hemisphere respectively. Thus

$$A_{FB}(\mathcal{P}_e, \mathcal{P}_{\bar{e}}) = \frac{3}{4} \left\{ \frac{\mathcal{A}_f [\mathcal{P}_{\bar{e}} - \mathcal{P}_e + \mathcal{A}_e(1 - \mathcal{P}_e \mathcal{P}_{\bar{e}})]}{1 - \mathcal{P}_e \mathcal{P}_{\bar{e}} + \mathcal{A}_e(\mathcal{P}_{\bar{e}} - \mathcal{P}_e)} \right\}. \tag{9.2.28}$$

This is a fundamental result and will be used to illustrate the power of utilising polarized beams. For the unpolarized asymmetry we have

$$A_{FB} = \frac{3}{4} \mathcal{A}_f \mathcal{A}_e. \tag{9.2.29}$$

Now recall that from (9.1.6) the vector coupling of the leptons is very small, so that the \mathcal{A}_l are also very small. Then for a given experimental error δA_{FB} we will have for the error on, say, \mathcal{A}_f

$$\delta \mathcal{A}_f \approx \frac{1}{\mathcal{A}_e} \delta A_{FB} \gg \delta A_{FB} \tag{9.2.30}$$

so that we cannot obtain a sufficiently accurate measurement of $\sin^2 \theta_W$.

On the contrary if we have, say, $\mathcal{P}_{\bar{e}} = 0$ but \mathcal{P}_e sizeable then

$$A_{FB}(\mathcal{P}_e) = -\frac{3}{4} \left\{ \frac{\mathcal{A}_f (\mathcal{P}_e - \mathcal{A}_e)}{1 + \mathcal{P}_e \mathcal{A}_e} \right\} \simeq -\frac{3}{4} \mathcal{A}_f \mathcal{P}_e. \tag{9.2.31}$$

In this case the error in $\delta\mathcal{A}_f$ will be comparable to that in A_{FB} :

$$\delta\mathcal{A}_f \approx \delta A_{FB}. \tag{9.2.32}$$

Again, the most advanced studies to date have been carried out at the Stanford SLC. The forward–backward asymmetry has been measured for $e^+e^- \rightarrow e^+e^-, \mu^+\mu^-, \tau^+\tau^-$, leading to (see Prepost, 1996)

$$\begin{aligned} \mathcal{A}_e &= 0.148 \pm 0.016 & \mathcal{A}_\mu &= 0.102 \pm 0.033 \\ \mathcal{A}_\tau &= 0.190 \pm 0.034, \end{aligned} \tag{9.2.33}$$

which are compatible with lepton universality.

When combined with the result (9.2.25) for A_{LR} these yield

$$\sin^2 \theta_W^{\text{eff}} = 0.23061 \pm 0.00047. \tag{9.2.34}$$

(iii) *Polarization of final state fermion for unpolarized e^-e^+*

If we are interested in the longitudinal polarization of the final state fermion f or in the final state correlations with a polarized initial state, we require the following additional CM reaction parameters:

- *the final fermion longitudinal polarizing power,*

$$\mathcal{P}_f(\theta) \equiv (00|Z0) = -\frac{\mathcal{A}_f(1 + \cos^2 \theta) + \mathcal{A}_e(2 \cos \theta)}{1 + \cos^2 \theta + \mathcal{A}_e\mathcal{A}_f(2 \cos \theta)} \tag{9.2.35}$$

$$= -\mathcal{P}_{\bar{f}}(\theta). \tag{9.2.36}$$

- *the final state correlation parameter,*

$$C_{ZZ} \equiv (00|ZZ) = -1, \tag{9.2.37}$$

again, a consequence of opposite helicities in the $f\bar{f}$ production;

- *the electron longitudinal depolarization parameter,*

$$\begin{aligned} D_{ZZ}(\theta) \equiv D_{ZZ}(e^-) \equiv (Z0|Z0) \\ = \frac{\mathcal{A}_e\mathcal{A}_f(1 + \cos^2 \theta) + 2 \cos \theta}{1 + \cos^2 \theta + \mathcal{A}_e\mathcal{A}_f(2 \cos \theta)} \end{aligned} \tag{9.2.38}$$

$$= D_{ZZ}(e^+); \tag{9.2.39}$$

- *the electron longitudinal polarization transfer parameter,*

$$\begin{aligned} K_{ZZ}(\theta) \equiv K_{ZZ}(e^-) \equiv (Z0|0Z) \\ = -D_{ZZ}(\theta) \end{aligned} \tag{9.2.40}$$

$$= K_{ZZ}(e^+); \tag{9.2.41}$$

- the three-spin and four-spin correlation parameters,

$$\begin{aligned} (Z0|ZZ) &= -(0Z|ZZ) \\ &= -A_Z(\theta) \end{aligned} \tag{9.2.42}$$

$$\begin{aligned} (ZZ|Z0) &= -(ZZ|0Z) \\ &= -\mathcal{P}_f(\theta) \end{aligned} \tag{9.2.43}$$

$$(ZZ|ZZ) = 1. \tag{9.2.44}$$

For an *unpolarized* initial state the degree of longitudinal polarization of the final fermion is given by (9.2.35), which in principle allows a determination of \mathcal{A}_f and \mathcal{A}_e if the longitudinal polarization of the final fermion can be measured.

If we assume lepton universality and take $\mathcal{A}_e = \mathcal{A}_f \approx 0.16$, corresponding to $\sin^2 \theta_W = 0.23$, then we see that $\mathcal{P}_f(\theta)$ varies from 0 at $\theta = \pi$ to about -30% at $\theta = 0$.

However, the measurement of $\mathcal{P}_f(\theta)$ requires an analysis of the angular distribution of the decay products of f (as discussed in subsection 8.2.1), which is a non-trivial matter.

It may therefore be better, from the point of view of statistics, to deal with an integrated quantity. Thus we define

$$\overline{\mathcal{P}}_f \equiv \frac{\int \mathcal{P}_f(\theta) d\sigma/d\Omega}{\int d\sigma/d\Omega}. \tag{9.2.45}$$

From the definition of $\mathcal{P}_f(\theta)$ in terms of relative numbers of right- or left-handed f particles produced at angle θ , it is clear that

$$\overline{\mathcal{P}}_f = \frac{\sigma(f_R) - \sigma(f_L)}{\sigma(f_R) + \sigma(f_L)} \tag{9.2.46}$$

where $\sigma(f_{R,L})$ are the total cross-sections to produce right- or left-handed f particles.

Using (9.2.35) and (9.2.12) in (9.2.45) we see that

$$\overline{\mathcal{P}}_f = -\mathcal{A}_f, \tag{9.2.47}$$

a beautiful and simple result.

In practice it appears that the most accurate results will come from $e^-e^+ \rightarrow \tau^-\tau^+$; the τ polarization can be studied via various decays, e.g. $\tau \rightarrow \pi\nu$, $\tau \rightarrow \mu\bar{\nu}_\mu\nu_\tau$, $\tau \rightarrow \rho\nu$, $\tau \rightarrow a_1\nu$.

(iv) *Measurement of the τ polarization*

We consider how the τ polarization can be measured. We work within the Standard Model where the τ is produced with longitudinal polarization and the neutrinos are purely left-handed ($\lambda_\nu = -1/2$). All the following results emerge as a straightforward application of the discussion of the

decay of unstable particles given in subsection 8.2.1, which should be consulted for notational conventions about angles etc.

(a) $\tau^- \rightarrow \pi + \nu_\tau$

Because $\lambda_\nu = -1/2$ and the π is spinless there is only one reduced helicity amplitude, (8.2.1). The decay is trivially magic and the normalized decay distribution of the π in the helicity rest frame of τ^- is given by (8.2.20) and (8.2.31):

$$W(\theta_\pi, \phi_\pi) = \frac{1}{\sqrt{4\pi}} \left[\frac{1}{\sqrt{4\pi}} + t_m^{1*} Y_{1m}(\theta_\pi, \phi_\pi) \right]$$

so that, using (3.1.35),

$$W(\theta_\pi) = \frac{1}{2} (1 + \mathcal{P}_\tau \cos \theta_\pi). \tag{9.2.48}$$

(b) $\tau^- \rightarrow V + \nu_\tau$, where V is a spin-1 meson (ρ or a_1)

There are now two independent reduced helicity amplitudes:

$$M(\lambda_V, \lambda_\nu)$$

with $\lambda_\nu = -1/2$ and $\lambda_V = 0$ or -1 . (The transition to $\lambda_V = +1$ is impossible by conservation of angular momentum.) Let us label these $M(0)$ and $M(-1)$ respectively. We can identify them by calculating the relevant helicity amplitudes $H_{\lambda_V \lambda_\nu; \lambda_\tau}$ with arbitrary choice of λ_τ and then using (8.2.1).

In the Standard Model the Feynman amplitude is given by

$$\frac{G}{2} \langle V; \lambda_V | h^\mu | 0 \rangle [\bar{u}_{\lambda_\nu} \gamma_\mu (1 - \gamma_5) u_{\lambda_\tau}] \tag{9.2.49}$$

where h^μ is the hadronic weak current and G is the Fermi coupling constant. (See, for example, Leader and Predazzi (1996), Chapter 1.) In (9.2.49) we have justifiably neglected the effects of the W propagator. We cannot, of course, calculate the hadronic matrix element $\langle V; \lambda_V | h^\mu | 0 \rangle$, but in any field theory it has to be proportional to the polarization vector $\epsilon^\mu(\lambda_V)$ of the spin-1 particle. Moreover the proportionality function is just a constant, since in the decay the momentum of V is fixed.

Using the fact that

$$\bar{u}_{-1/2}(v)(1 + \gamma_5) = 2\bar{u}_{-1/2}(v)$$

(see subsection 4.6.3), we can write

$$H_{\lambda_V \lambda_\nu; \lambda_\tau} = C \epsilon_\mu^*(\lambda_V) \bar{u}_{\lambda_\nu} \gamma^\mu u_{\lambda_\tau} \equiv C \epsilon_\mu^*(\lambda_V) V_{\lambda_\nu \lambda_\tau}^\mu \tag{9.2.50}$$

in the notation of subsection 4.6.2.

We can directly use the results (4.6.36)–(4.6.39) together with (4.6.30) and (4.6.28) to evaluate the amplitudes, taking for convenience the produced vector meson to have polar angles $\theta_V, \phi_V = 0$ in the helicity rest frame of

the τ . The only subtlety is to remember that the neutrino then has polar angles $\theta_\nu = \pi - \theta_V$, $\phi_\nu = \pi$.

For the polarization vector of the V meson, from (3.4.25), (3.4.24), (1.2.23) and (3.1.80), we have

$$\epsilon^{\mu*}(\pm 1) = \frac{1}{\sqrt{2}}(0, \mp \cos \theta_V, i, \pm \sin \theta_V) \tag{9.2.51}$$

and

$$\epsilon^{\mu*}(0) = \frac{1}{m_V}(p_V, E_V \hat{\mathbf{p}}_V), \tag{9.2.52}$$

where $\hat{\mathbf{p}}_V = (\sin \theta_V, 0, \cos \theta_V)$,

$$p_V = \frac{m_\tau^2 - m_V^2}{2m_\tau} \quad \text{and} \quad E_V = \frac{m_\tau^2 + m_V^2}{2m_\tau}. \tag{9.2.53}$$

After a little algebra involving the Pauli matrices in (4.6.30), one finds, up to a common constant,

$$\begin{aligned} H_{-1-1/2;1/2} &= -\sqrt{2} \sin \theta_V \\ H_{0-1/2;1/2} &= \frac{m_\tau}{m_V} \cos \theta_V. \end{aligned} \tag{9.2.54}$$

Comparing with (8.2.1), using

$$d_{1/2,-1/2}^{1/2}(\theta) = -\sin \theta/2$$

and

$$d_{1/2,1/2}^{1/2}(\theta) = \cos \theta/2$$

(see Appendix 1), we see that the correctly normalized reduced amplitudes are

$$M(0) = \frac{m_\tau}{\sqrt{m_\tau^2 + 2m_V^2}} \quad M(-1) = \frac{-\sqrt{2}m_V}{\sqrt{m_\tau^2 + 2m_V^2}}. \tag{9.2.55}$$

From (8.2.20), upon using (8.2.12) and (9.2.55) we find for the angular distribution of the vector meson

$$W(\theta_V) = \frac{1}{2} \left[1 + \left(\frac{m_\tau^2 - 2m_V^2}{m_\tau^2 + 2m_V^2} \right) \mathcal{P}_\tau \cos \theta_V \right]. \tag{9.2.56}$$

In practice, in order to use (9.2.48) or (9.2.56) to measure \mathcal{P}_τ we do not measure the angles θ_h ($h = \pi, \rho, a_1$) but convert the distribution into distributions in the Lab fractional energy $x_h \equiv E_h/E_\tau$ of the decay hadron, using

$$\cos \theta_h = \frac{2x_h - 1 - m_h^2/m_\tau^2}{1 - m_h^2/m_\tau^2}. \tag{9.2.57}$$

An example of the results from a measurement of $\mathcal{P}_\tau(\theta)$ by the L3 Collaboration at CERN (Acciarri *et al.*, 1994) is shown in Fig. 9.1. The curves correspond to fitting $\mathcal{P}_\tau(\theta)$ either with \mathcal{A}_τ and \mathcal{A}_e as independent parameters (no universality) or enforcing $\mathcal{A}_\tau = \mathcal{A}_e$ (universality). Excellent agreement with the Standard Model is obtained for a value $\sin^2 \theta_W^{\text{eff}} = 0.2309 \pm 0.0016$, nicely compatible with (9.2.26). For further experimental studies see: Delphi Collaboration, Abreu *et al.* (1995a, b); Aleph Collaboration, Buskulic *et al.* (1996) and OPAL Collaboration; Alexander *et al.* (1996).

(c) $\tau^- \rightarrow \rho^- + \nu_\tau$ with analysis of $\rho^- \rightarrow \pi^- \pi^0$

Additional information can be obtained by studying the angular distribution of say, π^- , in the $\rho^- \rightarrow \pi^- \pi^0$ decay. The theoretical analysis is a very nice example of the power of the methods discussed in subsection 8.2.1.

From (8.2.20) and (8.2.17) the angular decay distribution of the π^- , produced at an angle θ_π to the ρ 's direction of flight in the ρ helicity rest

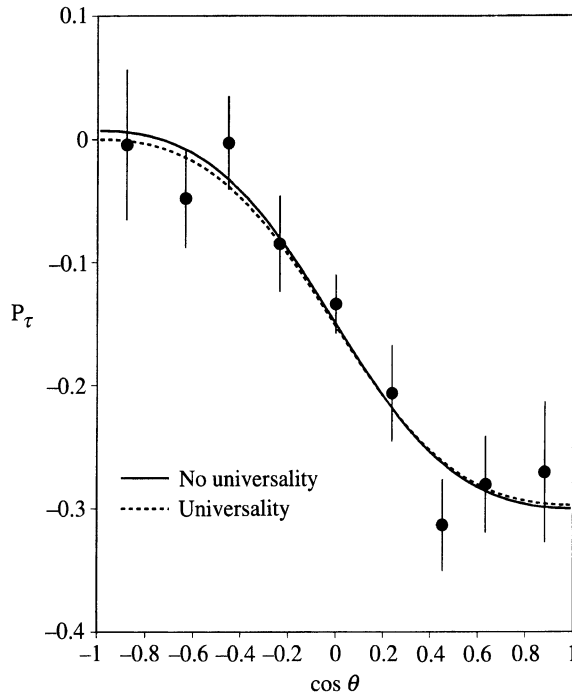


Fig. 9.1 The polarization $\mathcal{P}_\tau(\theta)$ vs. $\cos \theta$ for τ leptons produced in $e^-e^+ \rightarrow \tau^- \tau^+$ (from the L3 Collaboration, Acciarri *et al.* 1994). For a discussion of the two curves see the text.

frame is, after integration over the azimuthal angle ϕ_π ,

$$W(\theta_\pi) = \frac{1}{2} \left[1 - \sqrt{\frac{5}{2}} t_0^2(\rho, \theta_\rho) (3 \cos^2 \theta_\pi - 1) \right] \tag{9.2.58}$$

where $t_0^2(\rho, \theta_\rho)$ is the multipole parameter of the ρ , which was produced at angle θ_ρ in the τ helicity rest frame.

The experimental analysis of the π^- angular distribution is done in the ρ helicity rest frame reached from the Lab, where the π^- , π^0 are detected. Thus the Lab multipole parameters $t_0^2|_{S_L}$ needed in (9.2.58) will differ by a Wick rotation from the $t_0^2|_{S_\tau}$ of the ρ in the τ helicity rest frame.

From (3.2.9) and (2.2.5) the connection is

$$t_0^2(\rho, \theta_\rho) \Big|_{S_L} = d_{M0}^2(\theta_{\text{Wick}}) t_M^2(\rho, \theta_\rho) \Big|_{S_\tau} \tag{9.2.59}$$

in which, from (2.2.6), we have

$$\cos \theta_{\text{Wick}} = \gamma_\tau \frac{p_\rho + \beta_\tau E_\rho \cos \theta_\rho}{p_L^\rho} \tag{9.2.60}$$

$$\sin \theta_{\text{Wick}} = \gamma_\tau \beta_\tau \frac{m_\rho \sin \theta_\rho}{p_L^\rho} \tag{9.2.61}$$

where p_ρ and E_ρ are found from (9.2.53), p_L^ρ is the ρ Lab momentum and γ_τ , β_τ refer to the τ 's motion in the Lab.

To compute the $t_m^l(\rho)$ for the decay $\tau^- \rightarrow \rho^- + \nu_\tau$, in the τ helicity rest frame, we use (8.2.12), (8.2.14) and (9.2.55). It is easy to see that $t_2^2|_{S_\tau} = 0$. For the others we find

$$W(\theta_\rho) t_1^2(\rho, \theta_\rho) |_{S_\tau} = \frac{1}{2} \sqrt{\frac{3}{5}} \frac{m_\tau m_\rho}{m_\tau^2 + 2m_\rho^2} \mathcal{P}_\tau \sin \theta_\rho \tag{9.2.62}$$

$$W(\theta_\rho) t_0^2(\rho, \theta_\rho) |_{S_\tau} = -\frac{1}{2} \sqrt{\frac{2}{5}} \frac{1}{m_\tau^2 + 2m_\rho^2} \times \left[m_\tau^2 - m_\rho^2 + (m_\tau^2 + m_\rho^2) \mathcal{P}_\tau \cos \theta_\rho \right] \tag{9.2.63}$$

where $W(\theta_\rho)$ is found from (9.2.56).

Finally putting together (9.2.58)–(9.2.63), using the expressions for d_{M0}^2 given in Appendix 1, and eqn (9.2.56), we get for the normalized joint distribution for production of a ρ^- at angle θ_ρ , in the τ helicity rest frame, that then decays into a π^- at angle θ_π , in the ρ helicity rest frame reached from the Lab,

$$W(\theta_\rho | \theta_\pi) = \frac{1}{4} [f(\theta_\pi) + \mathcal{P}_\tau g(\theta_\rho, \theta_\pi)]. \tag{9.2.64}$$

Here

$$f(\theta_\pi) = 1 + \frac{m_\tau^2 - m_\rho^2}{m_\tau^2 + 2m_\rho^2} (3 \cos^2 \theta_\pi - 1) \tag{9.2.65}$$

and

$$\begin{aligned}
 g(\theta_\rho, \theta_\pi) &= (m_\tau^2 + 2m_\rho^2)^{-1} \\
 &\times \left\{ \left[m_\tau^2 - 2m_\rho^2 + \frac{1}{2}(m_\tau^2 + 2m_\rho^2)(3 \cos^2 \theta_\pi - 1)(3 \cos^2 \theta_{\text{Wick}} - 1) \right] \cos \theta_\rho \right. \\
 &\quad \left. + 3m_\tau m_\rho (3 \cos^2 \theta_\pi - 1) \sin \theta_{\text{Wick}} \cos \theta_{\text{Wick}} \sin \theta_\rho \right\} \tag{9.2.66}
 \end{aligned}$$

where it must be remembered that θ_{Wick} is a function of θ_ρ . Thus \mathcal{P}_τ can also be determined from an analysis of the two-dimensional distribution (9.2.64). Important comments about optimizing the statistical analysis of multi-dimensional distributions are given in Davier *et al.* (1993).

(d) $\tau^- \rightarrow a_1^- + \nu_\tau$, with analysis of $a_1^- \rightarrow 3\pi$

Further information is obtained if one studies the angular distribution of the normal \mathbf{n} (polar angles θ_n, ϕ_n) to the 3π decay plane in the a_1 helicity rest frame. (See subsection 8.2.2 for the three-body decays of an unstable particle.)

In general, as can be seen from (8.2.61) or from (8.2.78), for $a_1 \rightarrow$ three spin-0 particles, the angular distribution of the normal depends upon the *unknown* dynamical parameter $2R_{11} - 1$, which multiplies the $t_0^1(a_1)$ multipole parameter of the a_1 . However, for $a_1 \rightarrow 3\pi$, because of either identical-particle or isotopic-spin symmetry, the correctly symmetrized version of R_{11} vanishes after integration over the Dalitz plot; see (8.2.67).

Hence starting with (8.2.61) and using (8.2.62) we find the following result: after integration over the Dalitz plot, and after integrating over the azimuthal angle ϕ_n of the normal to the decay plane, the normalized angular distribution in θ_n is given by

$$\overline{W}(\theta_n) = \frac{1}{2} \left[1 + \frac{1}{2} \sqrt{\frac{5}{2}} t_0^2(a_1) (3 \cos^2 \theta_n - 1) \right], \tag{9.2.67}$$

very similar in form to (9.2.58).

Analogously to the case of $\rho \rightarrow 2\pi$, the decay pions in $a_1 \rightarrow 3\pi$ detected in the Lab will yield the distribution of \mathbf{n} in the helicity rest frame S_L reached from the Lab, so that a Wick rotation (9.2.59) must be carried out.

The result can be read off from the $\rho \rightarrow 2\pi$ case. One obtains

$$\overline{W}(\theta_{a_1} | \theta_n) = \frac{1}{4} [f'(\theta_n) + \mathcal{P}_\tau g'(\theta_{a_1}, \theta_n)] \tag{9.2.68}$$

where f' and g' are obtained from f and g in (9.2.65) and (9.2.66) by the substitutions

$$\begin{aligned} 3 \cos^2 \theta_\pi - 1 &\rightarrow \frac{1}{2}(1 - 3 \cos^2 \theta_n) \\ \theta_\rho &\rightarrow \theta_{a_1} & m_\rho &\rightarrow m_{a_1} \end{aligned} \tag{9.2.69}$$

(this must be done also inside θ_{Wick} ; see (9.2.60), (9.2.61)).

(e) *Correlation in $\tau^- \tau^+$ production*

The $\tau^- \tau^+$ are created in a correlated state in the $e^- e^+ \rightarrow \tau^- \tau^+$ reaction, so that further information can be obtained by studying the correlated decays of the τ^- and τ^+ .

There are two different approaches possible. We could write down from (8.2.22) the most general form for the joint angular distribution of the decay products, measure various correlation coefficients and then test whether their values correspond to the predictions of the Standard Model. We shall carry out, however, the somewhat simpler analysis of *assuming* the structure of the Standard Model and using the correlation analysis to measure the vector and axial-vector couplings, in effect, therefore, measuring $\sin^2 \theta_W$ by yet another method.

Because we are dealing with spin-1/2 resonances it is simpler to use the Cartesian spin formalism rather the multipole parameter language.

Firstly, for the production reaction, it is easy to see from (5.6.3), upon using the amplitudes given in (9.2.11), that the only non-zero expectation values are

$$\langle \sigma_Z(\tau^-) \rangle = \mathcal{P}_\tau = - \langle \sigma_Z(\tau^+) \rangle = -\mathcal{P}_{\bar{\tau}} \tag{9.2.70}$$

with \mathcal{P}_τ as given in (9.2.35),

$$\langle \sigma_Z(\tau^-) \sigma_Z(\tau^+) \rangle = -1 \tag{9.2.71}$$

and

$$\begin{aligned} \langle \sigma_X(\tau^-) \sigma_X(\tau^+) \rangle &= \langle \sigma_Y(\tau^-) \sigma_Y(\tau^+) \rangle \\ &= \left(\frac{v_\tau^2 - a_\tau^2}{v_\tau^2 + a_\tau^2} \right) \frac{\sin^2 \theta}{1 + \cos^2 \theta + 2 \mathcal{A}_e \mathcal{A}_\tau \cos \theta}. \end{aligned} \tag{9.2.72}$$

(Recall that the τ^- is produced at an angle θ to the e^- direction in the $e^- e^+$ CM; see (9.2.8).)

Secondly, we utilize (8.2.22); on the basis of (5.6.1) and (9.2.71), we substitute

$$\begin{aligned} t_{00}^{11}(\tau^-, \tau^+) &= \frac{1}{3} \langle \sigma_Z(\tau^-) \sigma_Z(\tau^+) \rangle = -\frac{1}{3} \\ t_{10}^{11} &= t_{01}^{11} = t_{11}^{11} = 0 \\ t_{1-1}^{11} &= t_{-11}^{11} = -\frac{1}{3} \langle \sigma_X(\tau^-) \sigma_X(\tau^+) \rangle. \end{aligned}$$

We can deal with all the negative decays $\tau^- \rightarrow \pi^- \nu_\tau, \rho^- \nu_\tau, a_1^- \nu_\tau$ and the positive decays $\tau^+ \rightarrow \pi^+ \bar{\nu}_\tau, \rho^+ \bar{\nu}_\tau, a_1^+ \bar{\nu}_\tau$ by writing the generic forms

$$\begin{aligned} W(\theta_-, \phi_-) &= \frac{1}{2}(1 + \alpha_- \mathcal{P}_\tau \cos \theta_-) \\ W(\theta_+, \phi_+) &= \frac{1}{2}(1 + \alpha_+ \mathcal{P}_{\bar{\tau}} \cos \theta_+) \end{aligned} \tag{9.2.73}$$

for their decay distributions with, from (9.2.48) and (9.2.56), and their analogues for τ^+ ,

$$\alpha_\pm(\pi) = \mp 1 \quad \alpha_\pm(V) = \mp \frac{m_\tau^2 - 2m_V^2}{m_\tau^2 + 2m_V^2} \tag{9.2.74}$$

where $V = \rho, a_1$.

For the normalized joint distribution we end up with

$$\begin{aligned} &W(\theta_-, \phi_-; \theta_+, \phi_+) \\ &= \frac{1}{16\pi^2} \left[1 + \alpha_- \mathcal{P}_\tau(\theta) \cos \theta_- + \alpha_+ \mathcal{P}_{\bar{\tau}}(\theta) \cos \theta_+ - \alpha_- \alpha_+ \cos \theta_- \cos \theta_+ \right. \\ &\quad \left. - 2\alpha_- \alpha_+ \left(\frac{a_\tau^2 - v_\tau^2}{a_\tau^2 + v_\tau^2} \right) \frac{\sin^2 \theta \sin \theta_- \sin \theta_+ \cos(\phi_- - \phi_+)}{1 + \cos^2 \theta + 2\mathcal{A}_e \mathcal{A}_\tau \cos \theta} \right] \end{aligned} \tag{9.2.75}$$

where the \mp angles are defined in the τ^-, τ^+ helicity rest frames respectively.

Clearly, the azimuthal dependence can be used to measure the parameter $(a_\tau^2 - v_\tau^2)/(a_\tau^2 + v_\tau^2)$, called C_{TT} in some of the experimental literature.

For experimental data see Abreu *et al.* (1997), where a value of $0.87 \pm 0.20 \pm 0.11$ was obtained, compatible with the value 0.978 corresponding to $\sin^2 \theta_W = 0.2236$.

(v) Polarization of final state fermion with polarized e^-e^+

As an example of the benefits of having polarized e^\pm beams, let us study the longitudinal polarization of the final state fermion f when the electron and positron have longitudinal polarizations $\mathcal{P}_e, \mathcal{P}_{\bar{e}}$ respectively.

From (5.6.3) and (5.6.5)

$$\begin{aligned} \mathcal{P}_f \frac{d\sigma}{d\Omega} \Big|_{\mathcal{P}_e, \mathcal{P}_{\bar{e}}} &= \frac{d\sigma}{d\Omega} [(00|Z0) + \mathcal{P}_e(Z0|Z0) + \mathcal{P}_{\bar{e}}(0Z|Z0) + \mathcal{P}_e \mathcal{P}_{\bar{e}}(ZZ|Z0)] \\ &= \frac{d\sigma}{d\Omega} [(1 - \mathcal{P}_e \mathcal{P}_{\bar{e}}) \mathcal{P}_f(\theta) + (\mathcal{P}_e - \mathcal{P}_{\bar{e}}) D_{ZZ}(\theta)] \end{aligned} \tag{9.2.76}$$

where $\mathcal{P}_f(\theta)$ is given by (9.2.35) and $D_{ZZ}(\theta)$ by (9.2.38). Substituting for

these yields

$$\mathcal{P}_f(\theta; \mathcal{P}_e, \mathcal{P}_{\bar{e}}) = -\frac{\mathcal{A}_f(1 + \gamma_1)(1 + \cos^2 \theta) + (\mathcal{A}_e + \gamma_2)2 \cos \theta}{(1 + \gamma_1)(1 + \cos^2 \theta) + \mathcal{A}_f(\mathcal{A}_e + \gamma_2)2 \cos \theta} \quad (9.2.77)$$

where $\gamma_{1,2}$ are given in (9.2.20).

The advantages of (9.2.77) are twofold. Firstly, by an appropriate choice of $\mathcal{P}_e, \mathcal{P}_{\bar{e}}$ we can obtain a much larger polarization. Figure 9.2 compares \mathcal{P}_f for unpolarized e^\pm with the case $\mathcal{P}_e = -\mathcal{P}_{\bar{e}} = 50\%$. This will enhance the asymmetry in the decay of, say, the τ . Secondly, it is useful from the point of view of statistics since one can use (9.2.77) to extract information from all f decays, no matter what the initial e^\pm polarizations are.

9.2.2 The reaction $e^-e^+ \rightarrow$ quark–antiquark pair

All the asymmetry measurements discussed in the previous section for $e^-e^+ \rightarrow$ lepton–antilepton pair can, in principle, be carried out for $e^-e^+ \rightarrow$

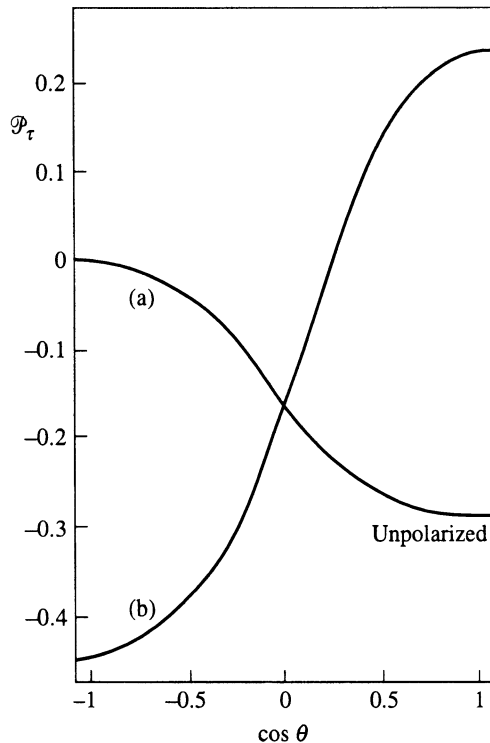


Fig. 9.2 Comparison of Standard Model τ polarization for e^-e^+ collisions: (a) unpolarized; (b) $\mathcal{P}_e = -\mathcal{P}_{\bar{e}} = 50\%$.

$q\bar{q}$. Thereby one is measuring the various vector and axial vector couplings v_f and a_f of (9.1.5) for the quarks.

(i) *Production of heavy quarks*

Experimentally the identification of a given quark and the determination of its direction of motion is much more complicated than for a lepton, and is probably only feasible for the b and c quarks. All sorts of tagging techniques are required as well as a determination of the thrust axis of the jet produced when the quark hadronizes.

We shall not attempt to cover this subject, but the reader is referred to Prepost (1996) for access to the literature.

The experimental complications are somewhat compensated by the large magnitude of the asymmetries compared with the lepton case. For the key parameters \mathcal{A}_i defined in (9.2.13) we have the following values for $\sin^2 \theta_W = 0.23$:

$$\begin{aligned} \mathcal{A}_e = \mathcal{A}_\mu = \mathcal{A}_\tau = 0.16 \quad \mathcal{A}_u = \mathcal{A}_c = \mathcal{A}_t = 0.67 \\ \mathcal{A}_d = \mathcal{A}_s = \mathcal{A}_b = 0.94. \end{aligned} \quad (9.2.78)$$

As a consequence the unpolarized forward–backward asymmetry (9.2.29) will be far larger for b and c quarks than for leptons.

For the polarized forward–backward asymmetry, with $\mathcal{P}_e = 0$ and $\mathcal{P}_e \approx 75\%$, (9.2.31) implies that $|A_{\text{FB}}^b| \approx 0.52$, a huge asymmetry.

Results for the parameters \mathcal{A}_b and \mathcal{A}_c vary somewhat according to the method used for tagging the quark but are essentially compatible with each other and with the Standard Model values. The world averages, given at the 1997 Lepton–Photon Conference (Timmermans, 1998) were

$$\mathcal{A}_b = 0.898 \pm 0.050 \quad \mathcal{A}_c = 0.649 \pm 0.058, \quad (9.2.79)$$

to be compared with the precise Standard Model predictions

$$\mathcal{A}_b^{\text{SM}} = 0.935 \quad \mathcal{A}_c^{\text{SM}} = 0.667. \quad (9.2.80)$$

Also, the polarization of the produced quark in an unpolarized e^+e^- collision will be very large and roughly independent of the production angle, as can be seen from (9.2.35):

$$\mathcal{P}_q(\theta) \approx -\mathcal{A}_q. \quad (9.2.81)$$

In principle the state of polarization of the heavy quark could be determined from the lepton energy spectrum in the semileptonic decay $b \rightarrow c + l + \bar{\nu}_l$. If we pretend that the quarks are free particles then this is analogous to the determination of the muon polarization from $\mu \rightarrow e\nu\bar{\nu}$ discussed in subsection 8.1.1(v). In reality one has to worry about the strong interaction effects, which lead to the hadronization of the quarks (see Mele, 1994). Interestingly, however, this will not be a problem for

top decay, if it were ever possible to produce $t\bar{t}$ pairs in lepton–antilepton collisions, since the decay is so rapid that there is no time for strong interaction effects to act.

(ii) *Production of light quarks*

By eqns (9.2.81) and (9.2.78) the u , d and s quarks are all produced with a high degree of polarization, but there is no sense in considering them as free particles and one is forced to take into account the process of *hadronization*, whereby the quark materializes as a physical particle. Since this is a non-perturbative strong interaction process we are unable to calculate it. The dynamics of the hadronization thus has to be studied experimentally. The focus, therefore, is not so much upon testing the electroweak theory as upon trusting the Standard Model to tell us about the state of the produced quark and then, by measuring the properties of the final state particles, to learn about the process of hadronization.

9.3 Summary

In summary, the measurement of spin-dependent observables has been and will continue to be a very powerful tool in testing the Standard Model to fantastic levels of precision. It is quite remarkable that the SLD measurement of A_{LR} using some 93 000 Z^0 events has achieved the same accuracy in the value of $\sin^2 \theta_W$ as all the LEP experiments put together, involving several million Z^0 events!